Catalysis Today 139 (2008) 88–93

Contents lists available at ScienceDirect

Catalysis Today

journal homepage: www.elsevier.com/locate/cattod

Al/Ce pillared clays with high surface area and large pore: Synthesis, characterization and supported palladium catalysts for deep oxidation of benzene

Shufeng Zuo, Qinqin Huang, Renxian Zhou *

Institute of Catalysis, Zhejiang University, Hangzhou 310028, PR China

ARTICLE INFO

Article history:
Available online 24 September 2008

Keywords:
Al/Ce pillared clays
Porous materials
Benzene catalytic oxidation
Pd catalyst

ABSTRACT

Large pore Al/Ce pillared clays (AlCe-PILC) were synthesized and used as supports for Pd catalysts in deep oxidation of low concentration of benzene (130–160 ppm). The supports and catalysts are characterized by X-ray powder diffraction (XRD), N_2 adsorption/desorption, high resolution transmission electron microscopy (HRTEM), energy dispersive X-ray spectroscopy (EDX) and temperature-programmed reduction techniques (TPR). The results showed that AlCe-PILC are characterized by basal spacings of 1.79–2.83 nm and have high surface areas of 343.6–377.4 m^2/g. Catalytic activity tests show that the catalytic activity of Pd catalysts in benzene deep oxidation is greatly dependent on the type of supports. Temperature for the complete benzene conversion using the following catalysts decreases in the order: Pd/Na-mmt (>400 °C) > Pd/Al-PILC (340 °C) > Pd/AlCe-PILC (≤300 °C). And the effects of hydrothermally treated time and different loading of Ce of Al/Ce pillaring solution on the activity of Pd/AlCe-PILC catalysts were also investigated, results of which show that high mesopore surface area and large pore structures of the supports are the key factors in improving the activity of the Pd/AlCe-PILC catalysts. The temperature for complete oxidation of benzene with Pd/AlCe-PILC (5;30) catalyst was 250 °C, exhibiting the highest catalytic activity.

1. Introduction

Volatile organic compounds (VOCs) emitted from industrial processes and automobile exhaust emissions are recognized as major contributions to air pollution because of their toxic properties and their involving in the formation of photochemical smog. Catalytic oxidation is one of the most important technologies used for the destruction of VOCs, especially when the VOC concentration is low, as it can treat the effluents at low/moderate temperatures, avoiding high energy costs [1–3]. Benzene, toluene, and xylene (BTX) are usually present in emissions due to solvent evaporation, coating operations, and thermal degradation of plastic materials. Because of its high toxicity, benzene allowable emission levels are significantly lower compared to other VOCs [4].

Several catalysts have been used for the total oxidation of benzene [5–12,4]. In general, noble metal catalysts are mainly for non-halogenated VOC destruction, while the metal oxide catalysts are used for halogenated VOCs [1]. Supported precious metals as Pt and Pd are well established as efficient catalysts for the oxidation of different VOC [13–15]. Moreover, among the precious metals, "Pd" is presently the cheapest one and "Pd" is often more active than "Pt" for oxidation [16]. The catalyst support used has most frequently been alumina because of its high specific surface area conducive to the dispersion of precious metals. It is well known that pillared clays have reached considerable interest as supports and catalysts over the past years. Their porosity, reactivity and thermal stability are being widely applied in adsorption and catalysis [17,18]. Pillared clays in general and pillared montmorillonite in particular are clay minerals that have been modified by introducing large polyoxycations into their interlayer regions. The separation between layers can be kept stable and depends on the polyoxycation used. The inorganic polyoxycations most frequently used as pillaring agents are species of aluminum, zirconium, titanium, chromium, and iron [19–23]. To prevent the clay layers from sintering at the high temperature of the catalytic reactions, the stability of the pillars must be increased. One way to achieve this is to introduce mixed pillars into the materials [24–27].

In this paper, a series of AlCe-PILC were synthesized by cation-exchange of with hydrothermally treated solutions with different Al/Ce molar ratios and hydrothermally treated time. Na-mmt, Al-PILC and AlCe-PILC supported Pd catalysts for the deep oxidation of low concentration of benzene were also investigated, and the supports and catalysts were characterized by XRD, N_2 adsorption/desorption, HRTEM, EDX, and H_2-TPR.

* Corresponding author. Tel.: +86 571 88273290; fax: +86 571 88273283.
E-mail address: zhourenxian@zju.edu.cn (R. Zhou).

0920-5861/$ – see front matter © 2008 Elsevier B.V. All rights reserved.
doi:10.1016/j.cattod.2008.08.026

2. Experimental

2.1. Preparation of supports and catalysts

Initial clay was a calcium montmorillonite with a composition of SiO_2 (58.84%), Al_2O_3 (16.41%), MgO (5.47%), CaO (2.72%), Fe_2O_3 (4.45%), Na_2O (0.07%) and K_2O (0.12%). The cation exchange capacity (CEC) of clay was 108.4 mequiv/100 g. Sodium form of the clay was obtained by addition of the clay to 1 M NaCl with constant stirring at 60 °C for 3 h, at the ratio of 0.1 L NaCl/1 g clay. The clay was then centrifuged and washed with deionized water repeatedly until free of chlorides, followed by drying at 110. This sample is labeled as Na-mmt.

Al/Ce pillaring solutions were prepared by hydrothermal treatment of a commercial solution of aluminium hydroxychloride (Locron L from Clariant, Switzerland) and $CeCl_3{\cdot}7H_2O$ solution. Hydrothermal treatments were carried out in Teflon coated stainless steel pressure vessels, which were slowly rotated for periods between 5 and 30 h at 130 °C. Al/Ce molar ratios of the pillaring solution was between 2.5 and 20, and concentration of Al was 2.5 M. After the conditions returned to room temperature and atmospheric pressure, the reaction mixture was diluted with the quantity of water necessary to yield an Al concentration of 0.1 M. Al pillaring solution was obtained from a 0.1 M Al solution from Locron L at room temperature.

The pillaring solutions with an Al/Na-mmt ratio of 20 mmol/g were added drop-wise to Na-mmt slurry of 2 g/0.1 L and then the reaction mixture was stirred continuously for 3 h at 60 °C, after which the mixture was filtered and washed with deionized water repeatedly until free of chlorides. Then the sample was dried at 110 °C and calcined at 500 °C for 2 h. These samples were labeled as Al-PILC and AlCe-PILC (*R*;*T*), where *R* and *T* represent Al/Ce molar ratio and hydrothermally treated time of the pillaring solutions respectively.

Pd/Na-mmt, Pd/Al-PILC and Pd/AlCe-PILC catalysts were prepared by an impregnation method with an aqueous of H_2PdCl_4 as metal precursors. The impregnated samples were reduced by hydrazine hydrate, then filtered and washed with a large amount of deionized water until free of chlorides, followed by drying at 110 °C and then calcination at 400 °C for 2 h. The content of Pd for all catalysts was 0.2 wt.%.

2.2. Characterization

Phase composition of the various samples was determined by means of XRD, using Rigaku D/max-3BX. Operating parameters were as follows: monochromatic Cu Kα radiation, Ni filter, 40 mA, 40 kV, 2θ values between 2° and 30°.

Textural properties of the samples were determined by nitrogen adsorption/desorption at liquid nitrogen temperature using a Coulter OMNISORP-100 apparatus. The samples were degassed under vacuum for 2 h at 250 °C before the measurements. Specific total surface area was calculated using the Brunauer–Emmett–Teller (BET) equation, whereas specific total pore volumes were evaluated from the nitrogen uptake at a relative N_2 pressure of $P/P_0 = 0.99$. The t-plot method was used to determine the mesopore surface area (A_{mes}) and Barrett–Joyner–Halenda (BJH) method to calculate the total pore volume.

Surface morphology analysis was carried out using HRTEM on JEM-2010 apparatus operated at 200 kV. Samples were prepared by epon embedding and ultra-thin sectioning. EDX analysis was performed on an OXFORD INCA instrument attached to the transmission electron microscope to find out the chemical composition.

The palladium content was determined by inductive couple plasma (ICP) after dissolution of the catalysts in a mixture of HF and HNO_3 solution. The result shows that for all the studied catalysts the palladium content is about 0.2 wt.%.

H_2-TPR was carried out in a flow system to observe reducibility of the supported Pd catalysts. Prior to H_2-TPR measurement, 50 mg catalyst was pre-treated in air at 300 °C for 0.5 h, and then the temperature was decreased to −30 °C. The reductive gas was a mixture of 5 vol.% H_2 in Ar (40 ml/min), which was purified using deoxidizer and silica gel. Temperature of the sample was programmed to rise at a constant rate of 10 °C/min. Amount of hydrogen uptakes during the reduction was measured by a thermal conductivity detector, and the effluent H_2O formed during H_2-TPR was absorbed with a 5 A molecular sieve. Hydrogen uptakes were quantified using CuO as a standard.

2.3. Catalytic activity tests

Benzene oxidation was carried out in a microreactor (quartz glass; 6 mm i.d., 8 mm o.d., WFS-3010, China) under atmospheric pressure at a space velocity of 20,000 h^{-1}. The reactive flow (125 ml/min) was composed of air and 130–160 ppm of gaseous benzene. Catalyst (0.3–0.35 g) was loaded in the quartz reactor with quartz wool packed at both ends of the catalyst bed, and the bed volume was about 0.375 ml. A thermocouple was placed in the center of catalyst bed to record reaction temperature and also to control the furnace. Benzene conversion in the effluent gas was analyzed by on-line gas chromatography. The products detected by mass spectrometry (QIC-20, HIDEN) were, only, CO_2 and H_2O. Thus, the conversion was calculated based on benzene consumption.

3. Results and discussion

3.1. Characterization

XRD diagrams between 2° and 30° (2θ) of Na-mmt, Al-PILC and AlCe-PILC (5;30) are presented in Fig. 1. From Fig. 1, it can be seen

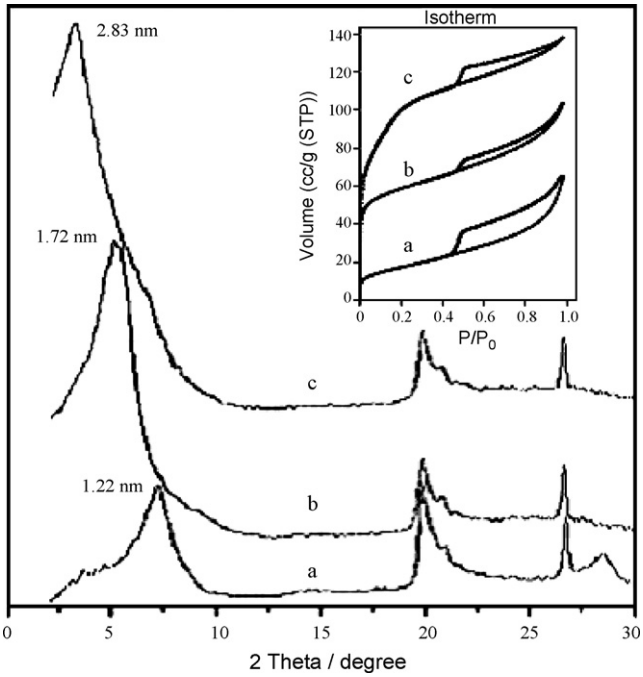

Fig. 1. XRD patterns and N_2 adsorption/desorption isotherms (inset) of (a) Na-mmt; (b) Al-PILC; (c) AlCe-PILC (5;30).

Table 1
Surface area, total pore volume, A_{mes} and basal spacing for all supports

Supports	BET surface area (m^2/g)[a]	Total pore volume (cm^3/g)[c]	A_{mes} (m^2/g)[b]	2θ (°)/Basal spacing (nm)
Na-mmt	61.9	0.1196	61.8	7.28/1.22
Al-PILC	202.8	0.1677	88.3	5.41/1.72
AlCe-PILC (5;5)	343.6	0.2270	127.4	4.82/1.83
AlCe-PILC (5;10)	354.6	0.2361	138.6	4.78/1.85
AlCe-PILC (5;20)	360.7	0.2287	206.5	4.16/2.12
AlCe-PILC (5;30)	366.4	0.2023	279.7	3.12/2.83
AlCe-PILC (2.5;30)	377.4	0.2440	136.5	4.86/1.82
AlCe-PILC (7.5;30)	371.2	0.2244	223.7	3.90/2.26
AlCe-PILC (10;30)	377.4	0.2421	199.5	4.26/2.07
AlCe-PILC (20;30)	372.8	0.2411	184.5	4.94/1.79

[a] Calculated by BET surface area.
[b] Calculated from the *t*-plot.
[c] Calculated from the BJH method.

that the $d_{0\,0\,1}$ spacing of Na-mmt is 1.22 nm, while the $d_{0\,0\,1}$ spacings of Al-PILC and AlCe-PILC (5;30) are 1.72 and 2.83 nm respectively. Shifting of 2θ values from 7.28° to 3.12° clearly suggests expansion of clay layer during pillaring process. 2θ angles at about 19.8° and 26.7° belong to cristobalite and quartz, respectively [28]. The $d_{0\,0\,1}$ spacing increased from 1.22 nm (Na-mmt) to 1.72 nm (Al-PILC) in the present case, indicating the presence of ion substituted Al_{13} ($[AlO_4Al_{12}(OH)_{24}(H_2O)_{12}]^{7+}$) like polymers. In contrast, AlCe-PILC (5;30) displayed a $d_{0\,0\,1}$ spacing at 2.83 nm, which is due to the fact that sizes of Al/Ce polyoxycations are larger than those of Al_{13}. Table 1 gives the basal spacing data for all the supports. As Table 1 indicated, compared to Al-PILC, AlCe-PILC have higher $d(0\,0\,1)$ values, which further indicates Al/Ce polyoxycations with sizes larger than those of Al_{13} between the clay layers when aluminum and cerium have been incorporated. It is interesting that the basal spacings of AlCe-PILC supports increase with the increase of the hydrothermally treated time of Al/Ce pillaring solution, which might be due to the polymeric degree of Al^{3+} and Ce^{3+} cations increases with the hydrothermally treated time increasing. However, too long hydrothermally treated time (>30 h) results in the formation of a white fibrous precipitate, which was identified with XRD as pseudoboehmite ($Al_{17}O_{16}(OH)_{16}Cl_3$). And the difference of Ce loading also results in the difference of $d(0\,0\,1)$ values. XRD pattern between 10° and 80° of AlCe-PILC (5;30) is displayed in Fig. 2, in which characteristic peaks of ceria phase were not observed, indicating the possibility that there was such a minor part of ceria outside the clay layers that it is indetectable by XRD. So it is suggested that most of ceria existed in the interlayer place.

Inset of Fig. 1 displays the N_2 adsorption/desorption isotherms for Na-mmt, Al-PILC and AlCe-PILC (5;30). It can be observed that adsorption of Na-mmt is very low. Al-PILC has a pronounced

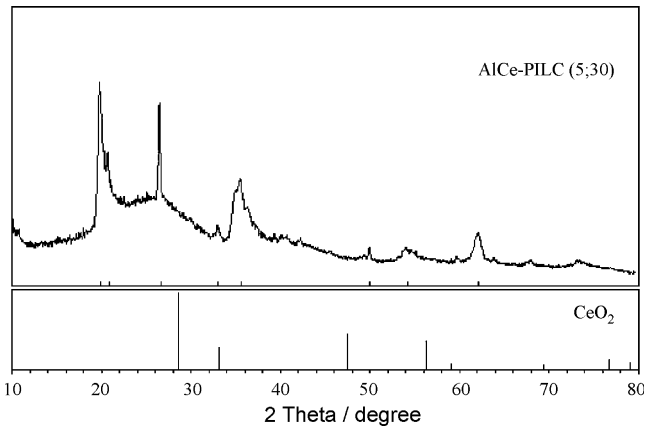

Fig. 2. XRD pattern between 10° and 80° of AlCe-PILC (5;30).

increase in porosity, and thus in adsorption, which is caused by the fact that polycations of aluminum hydrate were converted into alumina particles, forming rigid intercalated nanostructures. AlCe-PILC (5;30) exhibits the highest adsorption capacity, which is due to the formation of large Al/Ce polyoxycations, obtaining large pore structures.

BET surface area, total pore volume, and A_{mes} for all the supports are reported in Table 1. It can be observed that the surface area of Na-mmt increased from 61.9 to 202.8 m^2/g on Al-PILC and to 343.6–377.4 m^2/g on AlCe-PILC. Increase in surface area after pillaring is expected, since the process creates regular porosity [29]. After pillaring, the total pore volume increased from 0.1196 cm^3/g in Na-mmt to 0.1677 cm^3/g in Al-PILC and to 0.2023–0.2440 cm^3/g in AlCe-PILC. It is interesting that that A_{mes} of the supports correlates with the increase in basal spacings, especially for AlCe-PILC (5;30), A_{mes} of which reaches 279.7 m^2/g.

The XRD and N_2 adsorption/desorption results indicated that Al/Ce molar ratio and hydrothermally treated time of pillaring solution are the key factors in the preparation of large pore structures. McCauley [30] reported that at least 1 Ce atom has to be present per 52 Al atoms to obtain large pore pillared clay structures. Sterte [31] calculated that his large pore pillared clays had Al/La molar ratios ranging from 14 to 17. This may be explained by the presence of free La^{3+} in the interlayer due to excess La present in the starting solution (Al/La = 5). However, the large differences in the Al/Rare Earth molar ratios were observed in the large pore pillared clays by various authors.

The HRTEM images of Na-mmt and AlCe-PILC (5;30) are depicted in Fig. 3. It can be learned that Na-mmt has a layered structure and a two-dimension porous structure with small basal spacing. For AlCe-PILC (5;30) the layers were obviously kept apart, obtaining large pore structures, and the basal spacing between two neighboring fringes is about ←2.8 nm, corresponding to the $d_{0\,0\,1}$ spacing. Gandía et al. [32] reported that the intercalated polycations increase the basal spacing of the clays and, upon heating they are converted to metal oxide clusters by dehydration and dehydroxylation processes. These metal oxide clusters (pillars) between clay layers permanently keep apart the layers, generating an interlayer space of molecular dimensions. EDX spectrum clearly confirms the presence of Ce element, and XRD analysis of AlCe-PILC (5;30) at higher angles indicates no segregated ceria outside the interlayer region. So EDX result in reverse might prove the formation of Al/Ce mixed pillars between the clay layers.

Fig. 4 displays the TPR profiles associated with some catalysts and Table 2 gives hydrogen consumption and peak temperature. Blank experiments were carried out with bare supports under the same conditions and no H_2 consumption was observed. PdO is known to be an easily reducible oxide, even at room temperature, depending on the supports or precursors used in the preparation of

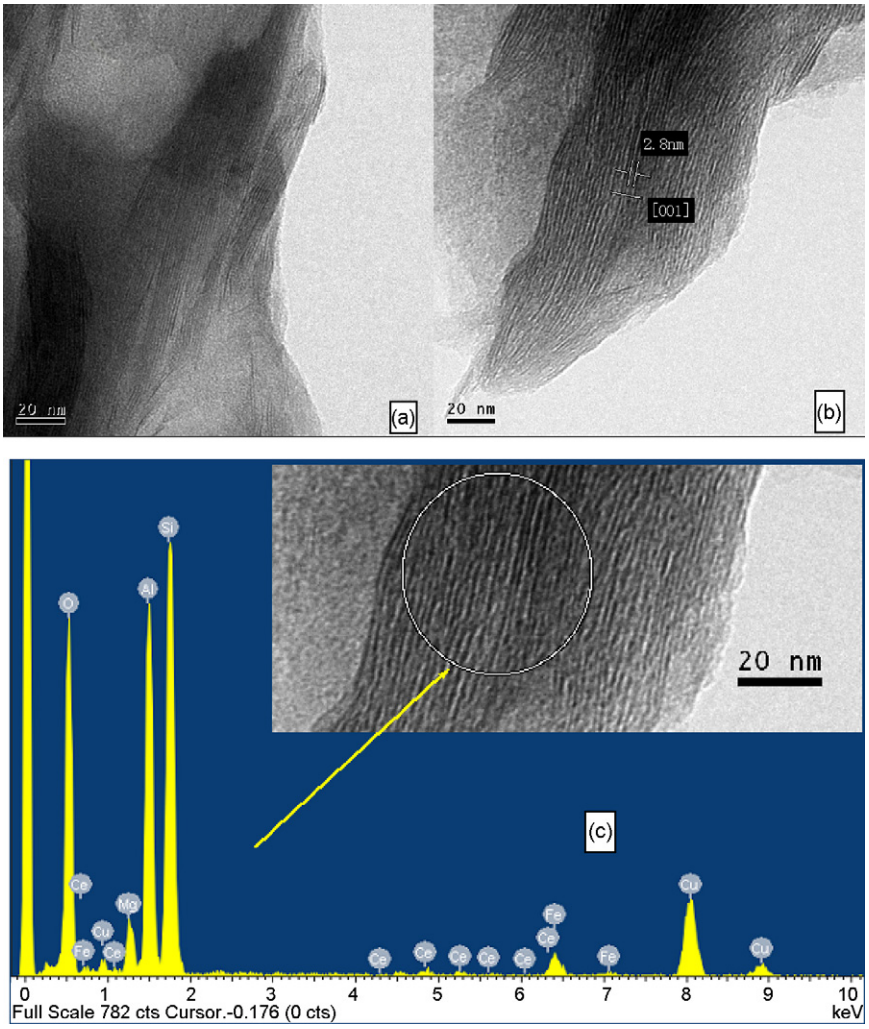

Fig. 3. HRTEM images of (a) Na-mmt; (b) AlCe-PILC (5;30); (c) EDX spectrum of AlCe-PILC (5;30), in which the Cu signals are from the grid used for HRTEM examination.

the catalysts [33–37]. For this reason, to ensure the detection of Pd reduction, TPR experiments were carried out starting at −30 °C by cooling the samples. Fig. 4 and Table 2 shows that the Pd/Na-mmt and Pd/Al-PILC catalysts exhibited two positive peaks (α and β) in the range of 0–150 °C, while Pd/AlCe-PILC (5;30) exhibits four peaks, followed by a reverse peak (γ). The two positive peaks can be attributed to the two-step reduction of PdO [38–41], which can be represented as follows:

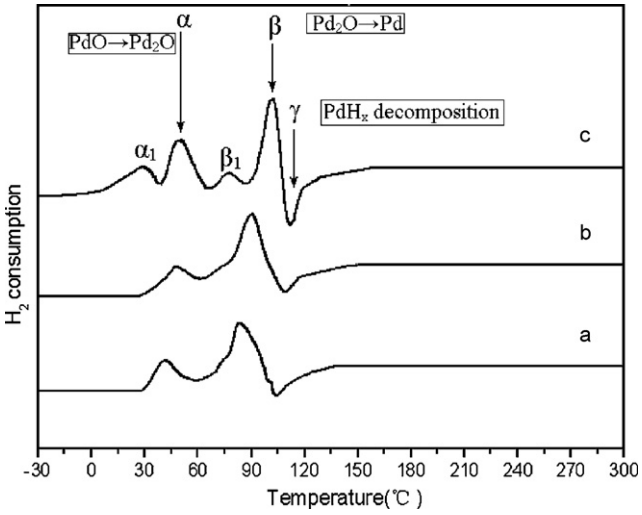

Fig. 4. TPR profiles of the catalysts: (a) Pd/Na-mmt; (b) Pd/Al-PILC; (c) Pd/AlCe-PILC (5;30).

$$2PdO + H_2 \rightarrow Pd_2O + H_2O \quad (1)$$

$$Pd_2O + H_2 \rightarrow 2Pd + H_2O \quad (2)$$

However, Pd_2O might already exist in the sample before reduction. Therefore, the second peak (β) might be attributed to Pd_2O, part of which was reduced from PdO and another part already existed before reduction. So the H_2 uptake for converting Pd_2O–Pd is higher than that for converting PdO–Pd_2O. And what's more, the total hydrogen consumption of Pd/Na-mmt and Pd/Al-PILC are about 16.1 and 17.8 μmol/$g_{cat.}$ respectively, which are lower than the amount (18.8 μmol/$g_{cat.}$) needed for stoichiometric reduction of PdO. The result proves that Pd_2O already existed before reduction.

The negative peak observed in the TPR profiles is characteristic of the palladium-containing catalysts, and it is attributed to the hydrogen desorption from decomposition of palladium hydride previously formed at low temperature. This phenomenon is in consistent with what previously observed by other authors [42,43].

Compared to Pd/Na-mmt, it is more difficult for Pd/Al-PILC to be reduced, as can be deduced from its profile. The higher temperature peaks may be due to the hydrogen consumed by

Table 2
H_2 uptake and temperature of TPR peaks for the catalysts

Catalysts	Peak α		Peak β	
	H_2 uptake ($\mu mol/g_{cat.}$)	Peak temperature (°C)	H_2 uptake ($\mu mol/g_{cat.}$)	Peak temperature (°C)
Pd/Na-mmt	2.96	40.2	13.1	83.9
Pd/Al-PILC	1.51	47.4	16.3	90.0
Pd/AlCe-PILC	7.53	49.7	12.7	102.6
	2.38 (Peak α_1)	27.9 (Peak α_1)	0.97 (Peak β_1)	77.6 (Peak β_1)

PdO_x species having stronger interaction with the support. For Pd/AlCe-PILC (5;30), the two peaks (α and β) observed at higher temperatures, compared to those of Pd/Al-PILC, may be due to the Pd–Ce interaction. It is well known that CeO_2 is an excellent promoter for noble metal-based combustion catalysts, the role of ceria being to act as phase-stabilizer for support, disperse and stabilize the metal in a more active form [44,45], so the peaks (α_1 and β_1) are attributed to the more greatly dispersed PdO_x species on AlCe-PILC (5;30).

Notably, the total hydrogen consumption of Pd/AlCe-PILC (5;30) catalyst is about 23.6 $\mu mol/g_{cat.}$, which exceeds the amount needed for stoichiometric reduction of PdO. This phenomenon is consistent with other reports, which concluded that the presence of Pd could decrease the temperature of surface ceria reduction by about 200 °C due to hydrogen activation by noble metals [46]. It is likely that this produces an accelerated diffusion of oxygen ions in the ceria interfaces from the bulk to the support surface and from the support to Pd particles, which promoted the reduction of Ce^{4+}. Furthermore, the increase in oxygen transfer on ceria interfaces can help maintain the PdO in a more cationic state. As a result, total H_2 consumption exceeded the amount needed for PdO reduction.

3.2. Catalytic activity and stability tests

The light-off curves of benzene deep oxidation over Pd catalysts are shown in Fig. 5. It can be concluded that the catalytic activity of Pd catalysts in benzene deep oxidation is greatly dependent on the type of supports. Gandía et al. [47] and Gil et al. [48] found also a marked influence of the characteristics of pillared clay supports on the activity of MnO_x and Pt catalysts for the deep oxidation of ketones. The activity of Pd supported on Na-mmt is very low, and temperature for the complete benzene conversion exceeds 400 °C. Pd supported on Al-PILC and AlCe-PILC catalysts present considerably higher activities than that on Na-mmt. The temperature for the complete benzene conversion decreases in the order: Pd/Na-mmt (>400 °C) > Pd/Al-PILC (340 °C) > Pd/AlCe-PILC (≤300 °C). This indicates that pillaring and addition of Ce are very important for the improving the activity of catalysts.

The hydrothermally treated time and different loading of Ce of Al/Ce pillaring solution obviously influence the activity of Pd/AlCe-PILC catalysts for benzene oxidation. Activity of the catalysts with different hydrothermally treated time decreases in the order: Pd/AlCe-PILC (5;30) > Pd/AlCe-PILC (5;20) > Pd/AlCe-PILC (5;10) > Pd/AlCe-PILC (5;5), and activity of the catalysts with different loading of Ce decreases in the order: Pd/AlCe-PILC (5;30) > Pd/AlCe-PILC (7.5;30) > Pd/AlCe-PILC (10;30) > Pd/AlCe-PILC (20;30) > Pd/AlCe-PILC (2.5;30). These orders are in accordance with the decreasing of basal spacing and A_{mes} of above supports. Kang et al. [49] reported supports with high surface area are feasible to obtain a large amount of exposed noble metal atoms even with a small loading. Xia et al. [50] reported the catalysts activity for aromatics oxidation is dependent on the pore size, as there is a smaller resistance for diffusion of reactants/products in and out of the larger pores, leading to higher catalyst activity. So we suggest that high A_{mes} and large pore structures of the supports are the key factors in improving the activity of Pd/AlCe-PILC catalysts for benzene deep oxidation. Temperature for complete oxidation of benzene with the catalyst of Pd/AlCe-PILC (5;30) was about 250 °C, exhibiting the highest catalytic activity.

The evolution with time-on-stream of benzene conversion at 300 °C for Pd/Na-mmt, Pd/Al-PILC and at 240 °C for Pd/AlCe-PILC (5;30) is reported in Fig. 6. It can be learned that the activity of the catalysts was measured within 24 h time-on-stream and during this period, no significant catalyst deactivation was observed. At temperatures of around 250 °C the benzene conversion efficiency with Pd/AlCe-PILC (5;30) remained above 99% and no deactivation of catalyst occurred after 100 h of operation. This result indicated

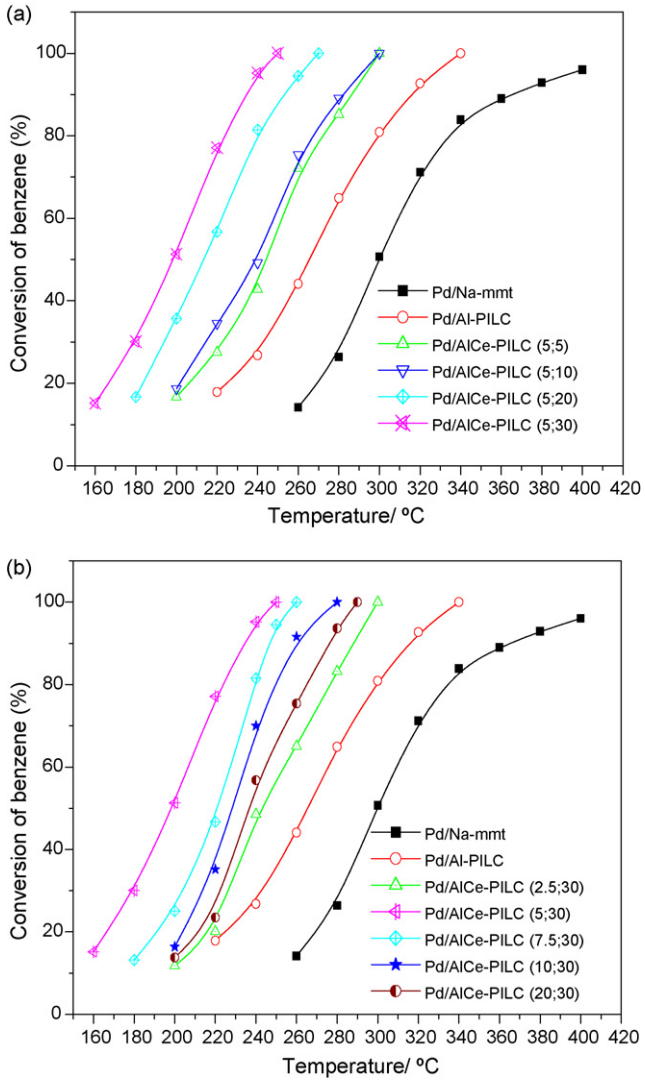

Fig. 5. Light-off curves for benzene deep oxidation over (a) Pd/Na-mmt, Pd/Al-PILC and Pd/AlCe-PILC (R = 5; T = 5,10,20,30); (b) Pd/Na-mmt, Pd/Al-PILC and Pd/AlCe-PILC (R = 2.5,5,7.5,10,20; T = 30).

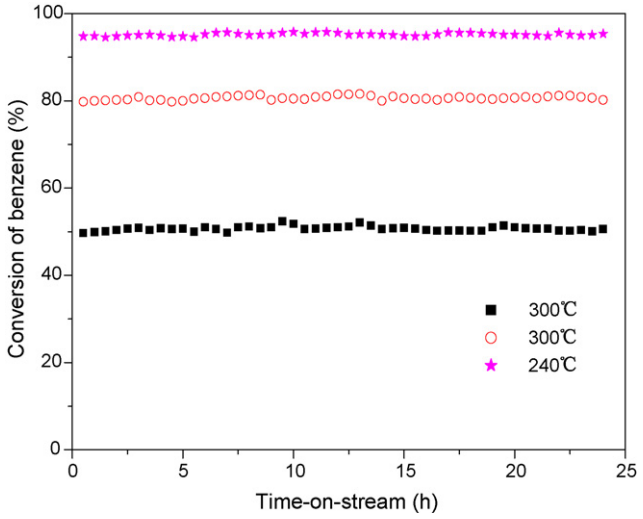

Fig. 6. Evolution of benzene conversion with time-on-stream for Pd/Na-mmt [■] at 300 °C, Pd/Al-PILC [○] at 300 °C and Pd/AlCe-PILC (5;30) [★] at 240 °C.

that in the present study, the Pd catalysts supported on different type of supports exhibit a good maintenance of catalytic activity.

4. Conclusions

Na-mmt, Al-PILC and a series of AlCe-PILC were synthesized and used as supports for Pd catalysts in deep oxidation of low concentration of benzene. The supports and catalysts were characterized by XRD, N_2 adsorption/desorption, HRTEM, EDX, and H_2-TPR. Basal spacings of Al-PILC and AlCe-PILC are 1.72 and 1.79–2.83 nm respectively, while that of Na-mmt is only 1.22 nm. BET surface areas of Al-PILC and AlCe-PILC are 202.8 and 343.6–377.4 m^2/g respectively, while that of Na-mmt is only 61.9 m^2/g. The above results suggest that the basal spacing is greatly enlarged and BET surface area is obviously increased after Al or Al/Ce pillaring. HRTEM images show that Na-mmt has a layered structure and a two-dimension porous structure with basal spacing small, while the layers of AlCe-PILC (5;30) were obviously kept apart, obtaining large pore structures. EDX analysis of Pd/AlCe-PILC (5;30) confirms the presence of Ce element, and the result in reverse proves the formation of Al/Ce mixed pillars between the clay layers. TPR profiles show that the Pd/Na-mmt and Pd/Al-PILC catalysts exhibited two positive peaks (α and β) in the range of 0–150 °C, while Pd/AlCe-PILC (5;30) exhibits four peaks, followed by a reverse peak (γ). The two positive peaks (α and β) can be attributed to the two-step reduction of PdO, and the negative peak is attributed to the hydrogen desorption from decomposition of a palladium hydride. The two peaks (α_1 and β_1) of Pd/AlCe-PILC (5;30) are attributed to the more greatly dispersed PdO_x species. Catalytic activity tests in benzene oxidation show the catalytic activity of Pd catalysts in benzene deep oxidation is greatly dependent on the type of supports. The temperature for complete benzene conversion decreases in the order: Pd/Na-mmt (>400 °C) > Pd/Al-PILC (340 °C) > Pd/AlCe-PILC (≤300 °C). This indicates that pillaring and addition of Ce are very important for improving the activity of catalysts. And the effects of hydrothermally treated time and different loading of Ce of Al/Ce pillaring solution on the activity of Pd/AlCe-PILC catalysts were also investigated, the results of which show that high A_{mes} and large pore structures of the supports are the key factors in improving the activity of the Pd/AlCe-PILC catalysts for benzene deep oxidation.

Acknowledgements

We gratefully acknowledge the financial supports from the Ministry of Science and Technology of China (No. 2004 CB 719504) and Nature Science Foundation of China (No. 20577043).

References

[1] J.J. Spivey, Ind. Eng. Chem. Res. 26 (1987) 2165.
[2] J.N. Armor, Appl. Catal. B 1 (1992) 221.
[3] J.J. Spivey, J.B. Butt, Catal. Today 1 (1991) 465.
[4] T.F. Garetto, C.R. Apesteguía, Appl. Catal. B 32 (2001) 83.
[5] S.K. Gangwal, M.E. Mullins, J.J. Spivey, P.R. Caffrey, B.A. Tichenor, Appl. Catal. 36 (1988) 231.
[6] M. Vassileva, A. Andreev, S. Dancheva, N. Kotsev, Appl. Catal. 49 (1989) 125.
[7] C. Lahousse, A. Bernier, P. Grange, B. Delmon, P. Papaefthimiou, T. Ionnides, X. Verykios, J. Catal. 178 (1998) 214.
[8] P. Papaefthimiou, T. Ioannides, X.E. Verykios, Appl. Catal. B 13 (1997) 175.
[9] P. Papaefthimiou, T. Ioannides, X.E. Verykios, Appl. Catal. B 15 (1998) 75.
[10] K.T. Chuang, A.A. Davydov, A.R. Sanger, M. Zhang, Catal. Lett. 49 (1997) 155.
[11] L. Becker, H. Forster, Appl. Catal. B 17 (1998) 43.
[12] R.S.G. Ferreira, P.G.P. de Oliveira, F.B. Noronha, Appl. Catal. B 29 (2001) 275.
[13] P. Dégé, L. Pinard, P. Magnoux, M. Guisnet, Appl. Catal. B 27 (2000) 17.
[14] J.C.-S. Wu, Z.-A. Lin, J.-W. Pan, M.-H. Rei, Appl. Catal. A 219 (2001) 117.
[15] J. Carpentier, J.-F. Lamonier, S. Siffert, E.A. Zhilinskaya, A. Aboukaïs, Appl. Catal. A 234 (2001) 91.
[16] J.R. González-Velasco, A. Aranzabal, J.I. Gutiérrez-Ortiz, R. López-Fonseca, M.A. Gutiérrez-Ortiz, Appl. Catal. B 19 (2000) 189.
[17] E. Kikuchi, T. Matstuda, Catal. Today 2 (1988) 297.
[18] I. Mrad, A. Ghorbel, D. Tichit, F. Lambert, Appl. Clay Sci. 12 (1997) 349.
[19] F. Figueras, Catal. Rev. Sci. Eng. 30 (1988) 457.
[20] D. Tichit, F. Fajula, F. Figueras, B. Ducouraut, G. Mascherpa, D. Gueguen, J. Bousquet, Clays Clay Miner. 36 (1988) 369.
[21] M.A. Martín-Luengo, H. Martins-Carvalho, J. Ladriere, P. Grange, Clay Miner. 24 (1989) 495.
[22] F. Figueras, A. Martrod-Bashi, G. Fetter, A. Therier, J.V. Zanchettr, J. Catal. 34 (1986) 658.
[23] B.M. Choudary, V.I.K. Valli, J. Chem. Soc. Chem. Commun. (1990) 1115.
[24] M.L. Ocelli, J. Mol. Catal. 35 (1986) 377.
[25] S.M. Bradley, R.A. Kydd, Catal. Lett. 8 (1991) 185.
[26] X. Tang, W.Q. Shu, Y.F. Shen, S.L. Suib, Chem. Mater. 7 (1995) 102.
[27] M.J. Hernando, C. Pesquera, C. Blanco, I. Benito, F. González, Chem. Mater. 8 (1995) 76.
[28] E. Booij, J.T. Kloprogge, J.A.R. van Veen, Appl. Clay Sci. 11 (1996) 155.
[29] S. Narayanan, K. Deshpande, Appl. Catal. A 193 (2000) 17.
[30] J.R. McCauley, U.S. Patent 4,818,737 (1988).
[31] J.P. Sterte, Clays Clay Miner. 39 (1991) 167.
[32] L.M. Gandía, M.A. Vicente, A. Gil, Appl. Catal. A 196 (2000) 281.
[33] Y.H. Chin, R. Dagle, J. Hu, A.C. Dohnalkova, Y. Wang, Catal. Today 77 (2002) 79.
[34] R. Ohnishi, W.L. Wang, M. Ichikawa, Appl. Catal. A 113 (1994) 10.
[35] N.S. Figoli, P.C. Largentiere, A. Arcoya, X.L. Seoane, J. Catal. 155 (1995) 95.
[36] N.W. Hurst, S.J. Gentry, A. Jones, Catal. Rev. Sci. Eng. 24 (1982) 233.
[37] L.M. Gómez-Sainero, X.L. Seoane, J.L.G. Fierro, A. Arcoya, J. Catal. 209 (1995) 279.
[38] B. Ngamsom, N. Bogdanchikova, M.A. Borja, P. Praserthdam, Catal. Commun. 5 (2004) 243.
[39] S. Fuentes, N. Bogdanchikova, M. Avalos-Borja, A. Boronin, M.H. Farías, G. Díaz, A.G. Cortes, A. Barrera, Catal. Today 55 (2000) 301.
[40] A. Barrera, M. Viniegra, P. Bosch, V.H. Lara, S. Fuentes, Appl. Catal. B 34 (2001) 97.
[41] K.-P. Sun, W.-W. Lu, M. Wang, X.-L. Xu, Appl. Catal. A 268 (2001) 107.
[42] A. Arcoya, X.L. Seoane, J. Soria, J. Chem. Technol. Biotechnol. 68 (1997) 171.
[43] R.M. Navarro, B. Pawelec, J.M. Trejo, R. Mariscal, J.L.G. Fierro, J. Catal. 189 (2000) 184.
[44] J. Kăspar, P. Fornasiero, M. Graziani, Catal. Today 50 (1999) 285.
[45] P.O. Thevenin, A. Alcalde, L.J. Pettersson, S.G. Järås, J.L.G. Fierro, J. Catal. 215 (2003) 78.
[46] R.S. Monteiro, F.B. Noronha, L.C. Dieguez, M. Schmal, Appl. Catal. A 131 (1995) 89.
[47] L.M. Gandía, M.A. Vicente, A. Gil, Appl. Catal. B 38 (2002) 295.
[48] A. Gil, M.A. Vicente, J.-F. Lambert, L.M. Gandía, Catal. Today 68 (2001) 41.
[49] T.G. Kang, J.-H. Kim, S.G. Kang, G. Seo, Catal. Today 59 (2000) 87.
[50] Q.-H. Xia, K. Hidajat, S. Kawi, Catal. Today 68 (2001) 255.